

# Investigation of the Rheological, Dynamic Mechanical, and Tensile Properties of Single-Walled Carbon Nanotubes Reinforced Poly(vinyl chloride)

M. Abu-Abdeen<sup>1,2</sup>

<sup>1</sup>Physics Department, College of Science, King Faisal University, Alhasa, Saudi Arabia

<sup>2</sup>Physics Department, College of Science, Cairo University, Giza, Egypt

Received 15 April 2011; accepted 9 June 2011

DOI 10.1002/app.35061

Published online 4 November 2011 in Wiley Online Library (wileyonlinelibrary.com).

**ABSTRACT:** Polymer nanocomposites consisting of single-walled carbon nanotubes (SWCNTs) and poly(vinyl chloride) were prepared by casting technique. The complex viscosity increased with increasing SWCNTs content, and it had a percolation concentration threshold equal to 0.45 wt % of SWCNTs. The storage modulus,  $G'$ , increased with increasing either SWCNTs content or frequency. A gradual decrease in the terminal zone slope of  $G'$  for the nanocomposites with increasing SWCNTs content may be explained by the fact that the nanotube–nanotube interactions will be dominant at higher CNTs content, and lead to the formation of the interconnected or network-like structures of SWCNTs in the polymer nanocomposites. The rheological loss factor indicates two relaxation peaks

at frequencies of 0.11 and 12.8 Hz due to the interaction between SWCNTs and polymer chains and glass transition, respectively. Dynamic mechanical properties were measured for the prepared composites. The results indicate that the storage modulus changes steadily, and the  $\tan\delta$  peaks are less intense for high SWCNTs content. Tensile tests were measured and depicted by an increase in the elastic modulus with increasing SWCNTs content, but it decreases for all composites as the testing temperature increased. © 2011 Wiley Periodicals, Inc. *J Appl Polym Sci* 124: 3192–3199, 2012

**Key words:** PVC; SWCNTs; DMA; nanocomposites; rheology; mechanical properties

## INTRODUCTION

Most of pristine polymers are relatively weak, as their cohesive energy is at least two orders of magnitude lower than that of inorganic materials. In recent years, there is an increased demand in the polymer industry for producing polymer composites that are stronger than those already on the market.<sup>1</sup> The physical properties of polymer can be improved by adding inorganic fillers. Many studies reported the effect of different inorganic fillers in the nano-scale on the polymer host properties. Poly(vinyl chloride) (PVC)/inorganic nanocomposites based on silica,<sup>2</sup> calcium carbonate,<sup>3</sup> montmorillonite (MMT),<sup>4</sup> titania<sup>6</sup> and calcium carbonate<sup>7,8</sup> have been previously reported.

As inorganic filler, carbon nanotube CNTs have many superior properties such as high aspect ratio, low weight, high thermal and electrical properties, and high elastic modulus. These properties make CNTs as a promising candidate for producing CNTs/polymer nanocomposites with multifunctional features.<sup>9–12</sup> The performance properties of

these types of composite can be related to the degree of association with the polymer, depending strongly on the composition of the CNTs, as determined by its nature.<sup>13</sup> Different polymer/CNTs nanocomposites have been synthesized by incorporating CNTs into various polymer matrices, such as polyamides,<sup>14</sup> polyimides,<sup>15–17</sup> epoxy,<sup>18</sup> polyurethane,<sup>19,20</sup> polypropylene,<sup>21–23</sup> and PVC.<sup>11</sup>

The rheological behavior of polymer nanocomposites as a function of filler content is of great importance in polymer processing, particularly for the analysis and design of processing operations, as well as understanding structure property relationships of polymer nanocomposites. The rheological behavior can realize the full potential of CNTs for application in thermoplastic matrix-based polymer nanocomposites and to optimize the processing conditions for achieving high performance polymer nanocomposites.<sup>24</sup>

Broza et al.<sup>25</sup> presented the general description of the nature of the glass transition temperature ( $T_g$ ) of polymers. Different experimental techniques, including differential scanning calorimetry, dynamic mechanical thermal analysis (DMTA), and dielectric measurements are used for the determination of  $T_g$ .<sup>26–28</sup> The influence of various low-dimension particles, for example, bismuth oxychloride and organic MMT, on the  $T_g$  of PVC was reported.<sup>29,30</sup> Generally, an increase of  $T_g$  as a function of nanoparticles

Correspondence to: M. Abu-Abdeen (mmaabdeen@yahoo.com or maboabdeen@kfu.edu.sa).

contained was found; however, for the MMT, an intercalation related decrease of  $T_g$  was stated.

In this study, rheological properties including the dependence of the complex viscosity, storage modulus, and loss factor of PVC reinforced with different concentrations of single-walled carbon nanotubes (SWCNTs) on frequency and SWCNTs content will be studied under isothermal conditions. The DMTA as a function of both CNTs content and temperature but at constant frequency will be also studied. The mechanical properties as a function of SWCNTs content and temperature will be studied through uniaxial tensile tests.

## EXPERIMENTAL

### Materials and preparation

Polyvinyl chloride (PVC) used in this work was supplied from Sabic Company (Saudi Arabia). It was in the powder form (powder fraction of 90–120  $\mu\text{m}$ , average size of 100  $\mu\text{m}$ , density  $\rho = 1.37 \text{ g/cm}^3$ ) was used as a polymeric matrix for preparation of composites. SWCNT (Aldrich 704113) with outer diameter of 0.7–1.3 nm and average length of 800 nm was purchased and used as it is to prepare the composites.

Initially, a desired amount of SWCNTs was dispersed in tetrahydrofuran (THF) solution. This solution was then sonicated for 30 min to obtain dispersive nanotubes suspension. The desired amount of PVC was also dissolved in THF. The weight ratio of SWCNTs in PVC was determined as follows. A fixed weights,  $w_p$ , of PVC and  $w_c$  of CNTs were chosen such that the total weight was  $w = w_p + w_c = \text{constant}$ . Then, the required ratio,  $w_c/w_p$ , was determined by varying both  $w_c$  and  $w_p$ . Both solutions were mixed together using a magnetic stirrer for 24 h to form SWCNTs solution mixture. The final mixture was further sonicated to give a black-colored stable solution with no detectable solid precipitation. The resulting solution was poured to betray dishes with fixed area and dried at room temperature. A series of composite films were prepared at different weight ratios (0.5–5 wt %) of SWCNTs/PVC. The film weight has to be very close to the fixed weight  $w$  to ensure the correct wt % of CNTs. The sample thickness was in the range of 0.09–0.11 mm.

### Testing

All tests in this study were carried out on a Dynamic Mechanical Analyzer (DMA) Q800 (TA Instruments LLC, Delaware) instrument with film clamps.

#### Tensile tests

The tensile tests were carried out on film specimens. The measurements were done at different temperatures of 22, 30, 40, 45, and 50°C at a force rate of

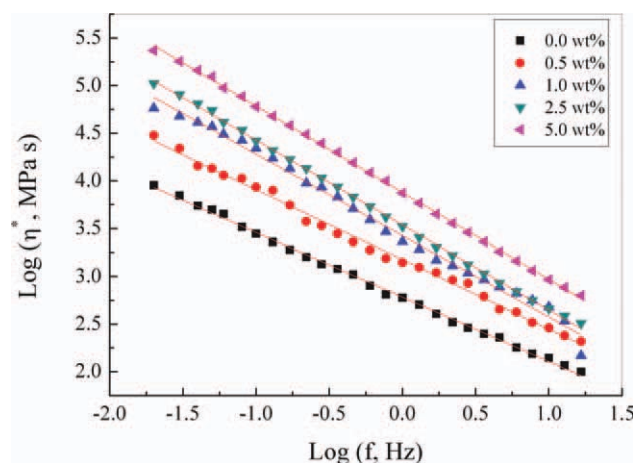


**Figure 1** The dependence of the complex viscosity on frequency for SWCNTs/PVC nanocomposites at room temperature. [Color figure can be viewed in the online issue, which is available at [wileyonlinelibrary.com](http://wileyonlinelibrary.com).]

1.5 N/min, according to ASTM D 412 and ASTM D 624, respectively.

#### Rheological and dynamic mechanical tests

The mentioned DMA Q800 instrument was used through the rheological and dynamic mechanical studies. For these tests, a film-clamp was used in dry mode. A slow heating rate of 1°C/min was used throughout to ensure that the sample was in thermal equilibrium with the instrument. The oscillating frequency was changed from 0.01 to 200 Hz.

Rheological tests experiments were performed with the film under tension, while the frequency is changed. A static preload force (0.01 N) was applied to the sample before the dynamic oscillating force to prevent film buckling.

During measurements, the instrument was programmed to maintain the static load at 125% of the force required to oscillate the sample. It is important that the film remained in its linear viscoelastic region during measurement (to ensure that the properties observed were independent of the deformation applied and truly reflected molecular motions), and so experiments were recorded maintaining constant strain. Generally, for thin polymer films, linear viscoelastic behavior can be assured with a strain less than 0.1%, and so this limit was used.

## RESULTS AND DISCUSSIONS

### Rheological properties

The complex viscosity,  $\eta^*$ , for PVC loaded with 0.0, 0.5, 1.0, 2.5, and 5.0 wt % SWCNTs as a function of frequency at constant temperature of 25°C is shown in Figure 1. Apparently, SWCNTs have a crucial

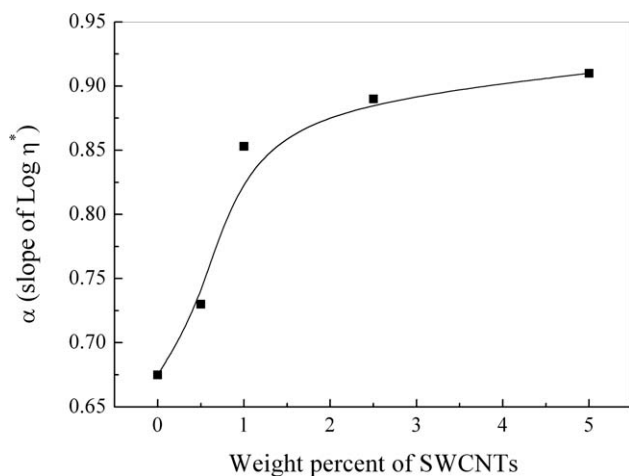


**Figure 2** The dependence of the slopes of the complex viscosity lines in Figure 1 on SWCNTs content at room temperature.

effect on the rheological behavior of the composites, even at low loadings. The complex viscosity increases with increasing SWCNTs content in the entire frequency range, but is more pronounced at low frequencies. At high frequencies, the impact of the carbon nanotubes on the rheological properties is definitely weaker, which suggests that the nanotubes do not significantly influence the short-range dynamics of the polymer chains. Generally, CNTs do affect polymer chain relaxation but with little effect on the local motion at short ranges.<sup>31</sup> The decrease in the complex viscosity with increasing frequency indicates a non-Newtonian behavior over the frequency range investigated. The complex viscosity can be expressed by an equation of the form

$$\text{Log}(\eta^*) = A - \alpha \text{Log}(f) \quad (1)$$

where  $A$  is a constant, and  $\alpha$  is the slope with values illustrated in Figure 2.

The dependence of  $\log(\eta^*)$  of the SWCNTs/PVC nanocomposites with the SWCNTs content at different frequencies of 0.02, 1.0, and 10 Hz is shown in Figure 3. It can be seen that  $\eta^*$  of the nanocomposites increased with increasing CNTs content over the frequency ranges investigated. In addition, the extent of increase in  $\eta^*$  with increasing SWCNTs content was more pronounced at low frequency when compared with that at high frequency. This increase in  $\eta^*$  with increasing SWCNTs content indicates an increase in physical interactions between the PVC matrix and the SWCNTs with high aspect ratio and large surface area. The increase in the complex viscosity of the studied nanocomposites with the SWCNTs was closely related to the increase in the storage modulus, which will be described in the following section.

The dependence of the complex viscosity on the concentration of SWCNTs (Fig. 3) appears to have what is known as rheological percolation behavior. To determine the rheological percolation threshold of CNTs-polymer composites, the relation between the complex viscosity and the concentration of the filler in a medium is drawn into a modified power law equation:

$$\eta^* \propto (m - m_c)^a \quad (2)$$

where,  $m$  is the CNTs' loading,  $m_c$  is the rheological percolation threshold and  $a$  is the critical exponents that depends on the oscillatory frequency.

In percolated systems one can observe a drastic change of the viscosity at a fixed frequency for a given concentration of the filler. This indicates that the CNT-polymer composite reaches a rheological percolation threshold at which the nanotubes block the motion of the polymer molecules. The power law eq. (2) was used to determine the value of the rheological percolation threshold. The function was fitted to the experimental data points of  $\eta^*$  at 0.02, 1.0, and 10 Hz for  $m > m_c$  (concentrations above percolation threshold). The scaling parameters were found by incrementally varying  $m_c$  until the best linear fit to the data points was obtained. The rheological percolation threshold ( $m_c$ ) was found to be at the SWCNTs concentrations of 0.45 wt % for all frequencies. Scaling exponent  $a = 0.85, 0.65,$  and  $0.55$  for frequencies 0.02, 1.0, and 10 Hz, respectively. The low rheological percolation threshold obtained in this study (0.45 wt %) is attributed to the high aspect ratio of the CNTs filler and indicates good and

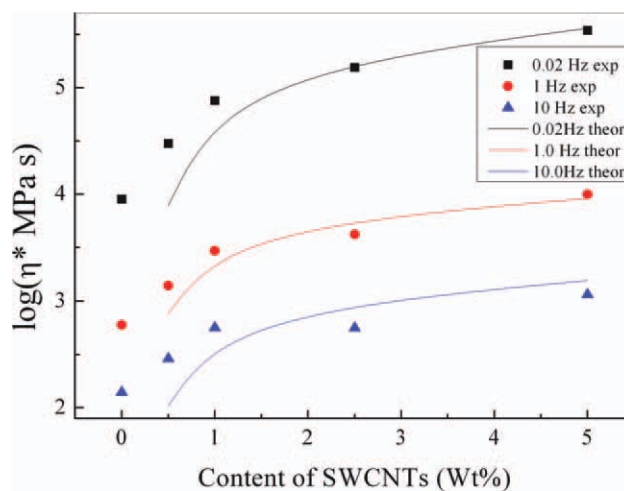


**Figure 3** The dependence of the complex viscosity on SWCNTs content at different frequencies of 0.02, 1.0 and 10 Hz at room temperature. [Color figure can be viewed in the online issue, which is available at [www.interscience.wiley.com](http://www.interscience.wiley.com).]



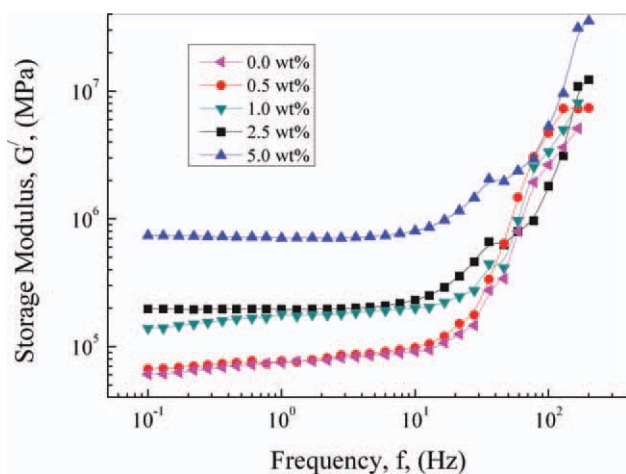


**Figure 4** The dependence of the storage modulus on frequency for SWCNTs/PVC nanocomposites at room temperature. [Color figure can be viewed in the online issue, which is available at [wileyonlinelibrary.com](http://wileyonlinelibrary.com).]

homogenous dispersion of SWCNTs within PVC matrix.

The storage modulus,  $G'$ , of the SWCNTs/PVC nanocomposites as a function of frequency at constant temperature of 25°C is shown in Figure 4. The figure can be divided into two regions separated by a frequency  $f_r$  ( $= 10$  Hz), implying two mechanisms. At frequencies greater than  $f_r$ , the storage modulus  $G'$  of the SWCNTs/PVC nanocomposites markedly increased with increasing frequency and SWCNTs content, where this increment being more significant at low frequency. This rheological response is similar to the relaxation behavior of the typical filled-polymer composite systems.<sup>24,32</sup> A gradual decrease in the terminal zone slope of  $G'$  for the nanocomposites with increasing SWCNTs content may be explained by the fact that the nanotube–nanotube interactions will be dominant at higher CNTs content and lead to the formation of the interconnected or network-like structures of SWCNTs in the polymer nanocomposites. At frequencies lower than  $f_r$ , the storage modulus is slightly increased with increasing CNTs content while for samples containing 5 wt % CNTs,  $G'$  seems to be frequency independent. This may be explained by the fact that the nanotube–nanotube interactions increased with increasing SWCNTs content and led to the formation of the interconnected or network-like structures of SWCNTs in the polymer nanocomposites, resulting in the pseudosolid-like behavior.

The change in the storage modulus of the SWCNTs/PVC nanocomposites as a function of SWCNTs content at constant temperature of 25°C is shown in Figure 5. The storage modulus increases markedly with increasing SWCNTs content. This increases perhaps because the SWCNTs can be more easily dispersed effectively in the PVC matrix, caus-

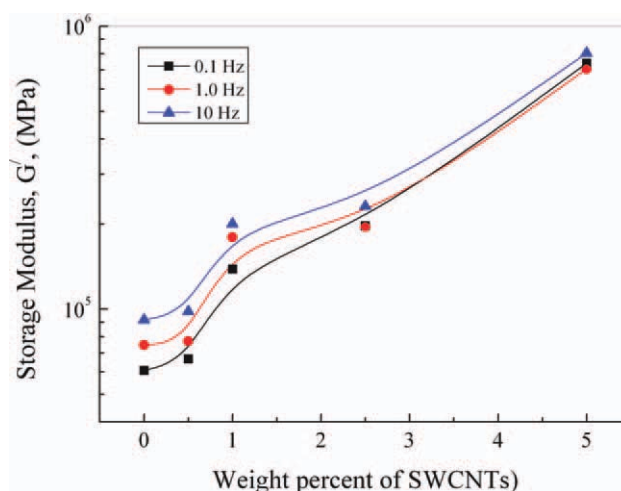


**Figure 5** The dependence of the storage modulus on SWCNTs content at different frequencies of 0.1, 1.0 and 10 Hz at room temperature. [Color figure can be viewed in the online issue, which is available at [wileyonlinelibrary.com](http://wileyonlinelibrary.com).]

ing strong interactions. On the other hand,  $G'$  slightly increases with frequency at low CNTs loadings while there is no, approximately, changes at higher CNTs loadings. At this configuration, interactions between CNTs and polymer chains may restrict the motion of these chains.

The loss factor,  $\tan\delta$ , of the SWCNTs/PVC nanocomposites as a function of frequency at constant temperature of 25°C is shown in Figure 6. The figure shows two relaxation peaks at frequencies of 0.11 and 12.8 Hz. The peaks heights increase with increasing SWCNTs content. The first peaks that appear at low frequency are due to the interaction between CNTs and polymer chains. The  $\tan\delta$  maximum  $(\tan\delta)_{\max}$  are seen to shift toward lower

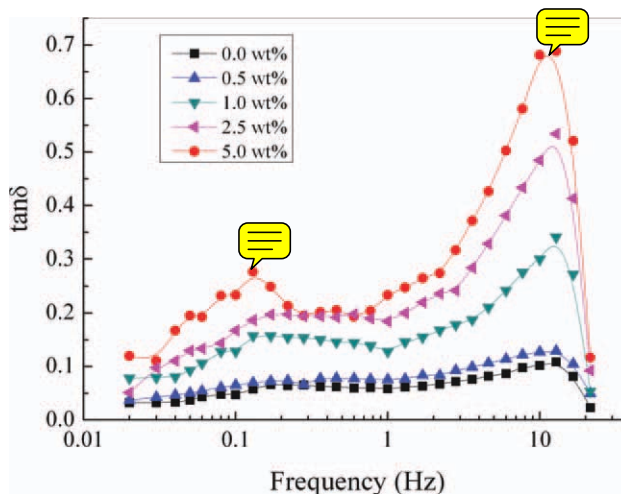


**Figure 6** The dependence of the loss factor  $\tan\delta$  on frequency for SWCNTs/PVC nanocomposites at room temperature. [Color figure can be viewed in the online issue, which is available at [wileyonlinelibrary.com](http://wileyonlinelibrary.com).]

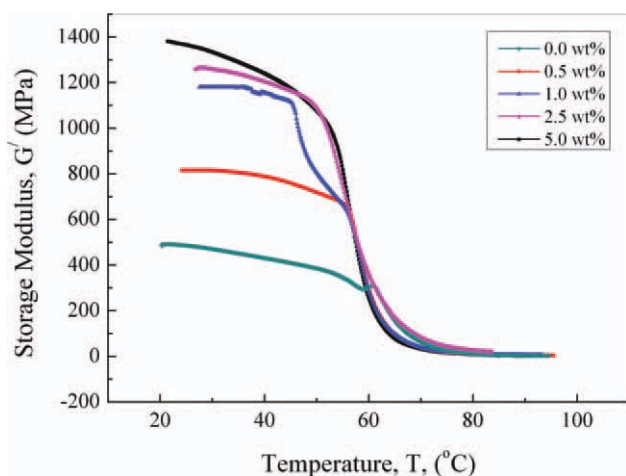


**Figure 7** The dependence of the storage modulus on temperature for SWCNTs/PVC at a frequency of 3.0 Hz at room temperature. [Color figure can be viewed in the online issue, which is available at [wileyonlinelibrary.com](http://wileyonlinelibrary.com).]

frequency with increasing SWCNTs content as a result of the more efficient blocking effect of CNTs leads to suggest that the mobility of polymer chains is hindered by the nanotubes. On the other hand, the peaks appear at high frequency are due to the glass transition.<sup>33</sup> At high frequency values, the trend observed for pristine PVC and nanocomposites indicates that motions across entanglements are possible despite the presence of nanotubes.

### Dynamic mechanical properties

Figure 7 plots the storage modulus  $G'$  of SWCNTs/PVC nanocomposites, obtained by DMA measurement, as a function of temperature at a constant frequency of 3 Hz. A single mechanical transition has

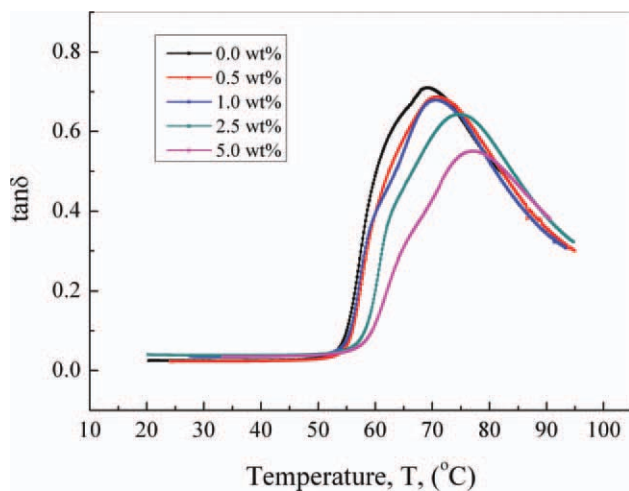


**Figure 8** The dependence of the loss factor  $\tan\delta$  on temperature for SWCNTs/PVC at a frequency of 3.0 Hz at room temperature. [Color figure can be viewed in the online issue, which is available at [wileyonlinelibrary.com](http://wileyonlinelibrary.com).]

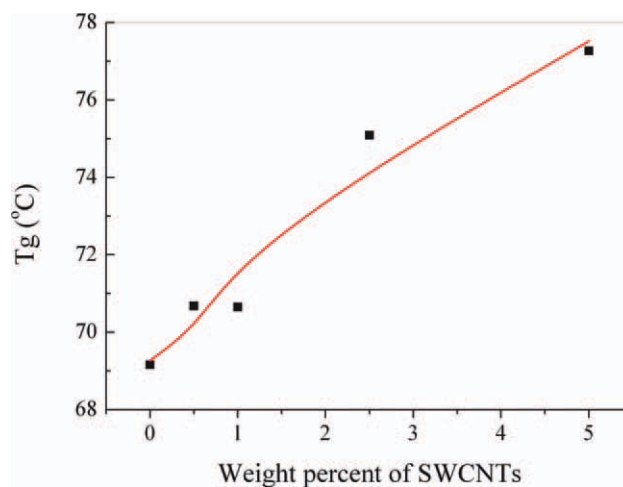


**Figure 9** The dependence of the  $T_g$  on SWCNTs content at frequency of 3.0 Hz at room temperature. [Color figure can be viewed in the online issue, which is available at [wileyonlinelibrary.com](http://wileyonlinelibrary.com).]

been observed in the temperature range studied and is recognized as the  $\alpha$ -relaxation or the glass transition peak. The  $\alpha$ -relaxation is related to the Brownian motion of the main chain associated with the glass transition and the relaxation of segments associated with it. Onset of glass transition is marked by a sharp decrease in its storage modulus, as shown in Figure 7.

The  $T_g$  of a polymer is usually taken from the peak position of loss modulus or  $\tan\delta$  versus temperature curves. Peaks of  $\tan\delta$  are typically found at somewhat higher temperatures depending on the intensity and/or width of the transition. Figure 8 presents the change of  $\tan\delta$  versus temperature for all studied nanocomposites at a frequency of 3 Hz. Adding SWCNTs to the PVC matrix shifts the  $\tan\delta$

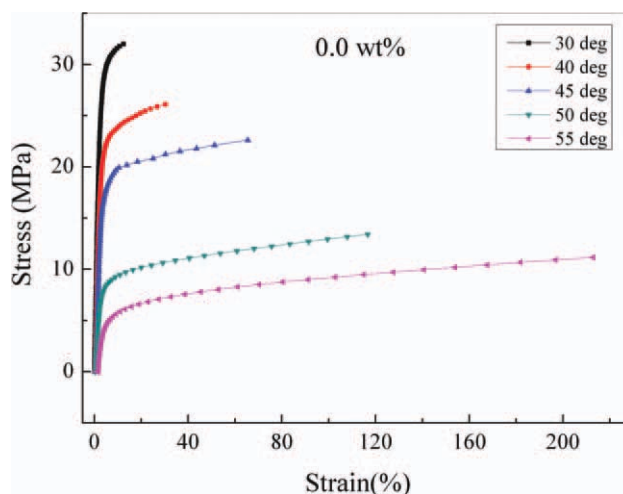


**Figure 10** Stress–strain curves for the pristine PVC at different testing temperatures. [Color figure can be viewed in the online issue, which is available at [wileyonlinelibrary.com](http://wileyonlinelibrary.com).]

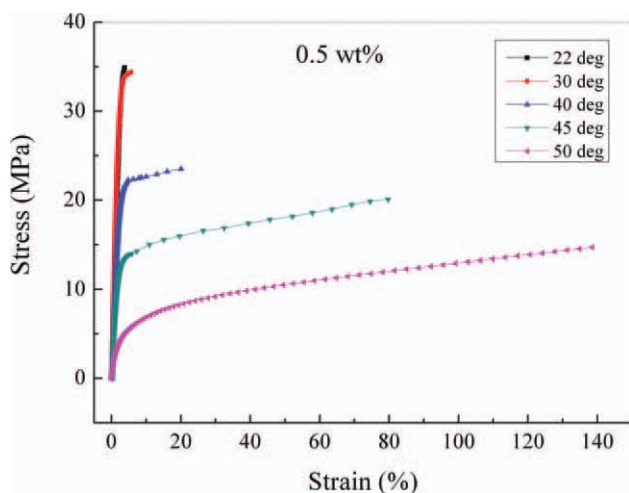


**Figure 11** Stress–strain curves for 0.5 wt % reinforced PVC at different testing temperatures. [Color figure can be viewed in the online issue, which is available at [wileyonlinelibrary.com](http://wileyonlinelibrary.com).]

peak values of these composites to high temperature regions, implying an interaction between CNTs and the PVC molecules. Increasing the CNTs content also lowers the  $\tan \delta$  peak intensity. The height of the  $\tan \delta$  peak measures the energy-damping characteristics of a material. The damping of  $\tan \delta$  intensity is a good indicator of a well dispersion of CNTs in the polymer matrix, so they directly enhance the stiffness of the composites.

Figure 9 plots the relationship between the  $T_g$  of SWCNTs/PVC nanocomposites and SWCNTs at a frequency of 3 Hz. All the  $T_g$  values of the studied nanocomposites increased with the CNTs content. The  $T_g$  of the SWCNTs/PVC nanocomposites increases from 69.16 to 77.27°C as SWCNTs from 0

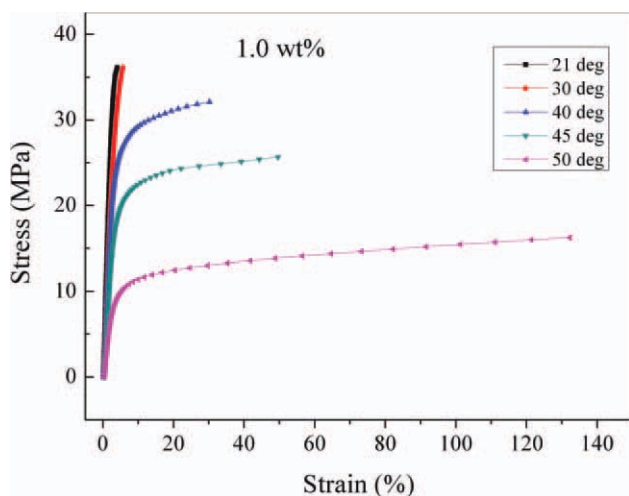


**Figure 12** Stress–strain curves for 1.0 wt % reinforced PVC at different testing temperatures. [Color figure can be viewed in the online issue, which is available at [wileyonlinelibrary.com](http://wileyonlinelibrary.com).]

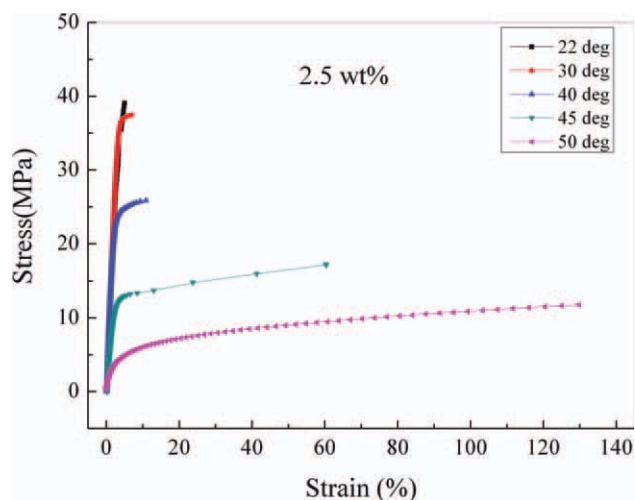


**Figure 13** Stress–strain curves for 2.5 wt % reinforced PVC at different testing temperatures. [Color figure can be viewed in the online issue, which is available at [wileyonlinelibrary.com](http://wileyonlinelibrary.com).]

to 5 wt %, respectively. The interfacial interactions between the CNTs and PVC molecules are strong; so,  $T_g$  of these nanocomposites increased with the polymer restriction of the chains by the CNTs and also by the good dispersion of CNTs in the PVC matrix.

### Tensile properties

Figures 10–14 present the stress–strain curves for PVC loaded with 0, 0.5, 1.0, 2.5, and 5.0 wt % of SWCNTs at different temperatures of 22, 30, 40, 45, and 50°C, respectively. The maximum stress reached in these Figures is not the ultimate strength, but it is the maximum stress available for the instrument

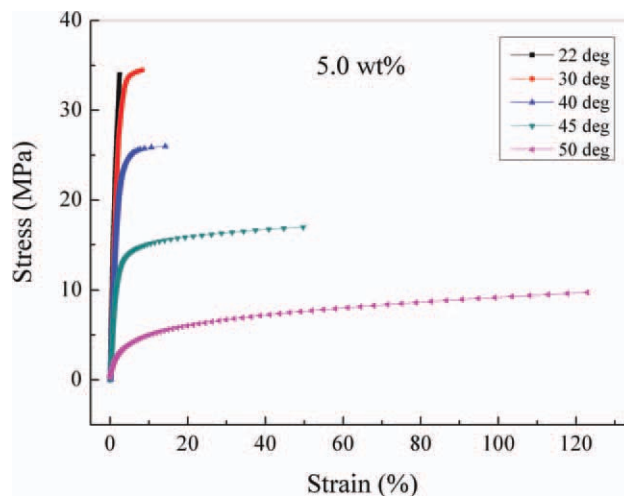


**Figure 14** Stress–strain curves for 5.0 wt % reinforced PVC at different testing temperatures. [Color figure can be viewed in the online issue, which is available at [wileyonlinelibrary.com](http://wileyonlinelibrary.com).]



**TABLE I**  
The Calculated Values of Both Yield Stress and Yield Strain as a Function of SWCNTs Content and Temperature

SWCNTs content (wt %)	Yield stress (MPa)				Yield strain (%)			
	30°C	40°C	45°C	50°C	30°C	40°C	45°C	50°C
0.0	24.6	19.9	9.8	7.9	4.28	4.9	4.9	5.4
0.5	34.5	22.4	15.2	8.9	2.2	2.6	3.7	4.4
1.0	–	29.8	23.6	12.7	–	5.2	5.2	3.7
2.5	36.4	24.8	14.1	7.8	2	2.8	3.1	3.4
5	38	26.1	17	10	2.5	3.9	3.5	5.5

used. All composites at temperatures 22, 30, 40, and 45°C show at first straight lines relations between stress and strain in the studied range of stresses. This reflects the Hookean behavior of these composites at these temperatures. At a temperature of 50°C (which is near the  $T_g$  of PVC prepared by casting technique), yielding of these materials takes place with yield stress and yield strain values as listed in Table I.

The linear Hookean regions at low strains below the yield strain are used to calculate the elastic modulus,  $E$ , for all composites at the different temperatures investigated. Figure 15 plots a relation between the calculated values of the elastic modulus and the weight percent of SWCNTs content at 22°C. The elastic modulus is found to increase linearly with SWCNTs content according to the equation:

$$E = E_o + b C \quad (3)$$

where  $E_o$  is the elastic modulus of the pristine PVC and  $b$  is the slope and equals to 207 MPa. This increase in  $E$  implies a good dispersion of SWCNTs inside the polymer matrix, which increases the interfacial interaction between the CNTs and the polymer

chains. This interaction increases as the amount of added CNTs increased. This result is in consistent with the results obtained for the storage modulus. As the testing temperature increased, polymer chains may be activated and some of them overcome the hindering effect made by SWCNTs and tend to reorient themselves to a new configuration in a manner that reduces the elastic modulus as shown in Figure 16 for all studied composites. The lines in this figure obey the equation

$$E(T) = E'_o - m(T - T_o) \quad (4)$$

where  $E'_o$  is the elastic modulus at temperature  $T_o$  and  $m$  is the slope and equals to 34.1, 34.5, 41, 46.8, and 49.7 MPa/deg for samples containing 0.0, 0.5, 1.0, 2.5, and 5 SWCNTs wt % content, respectively. It is noticed that the values of  $m$  is high for high SWCNTs loadings. As stated before, high loadings of CNTs means more interfacial interaction between them and polymer chains which act as obstacles for chains mobility. So, as the testing temperature increased more obstacles may overcome, resulting in more reorientations of polymer chains. Thus, the

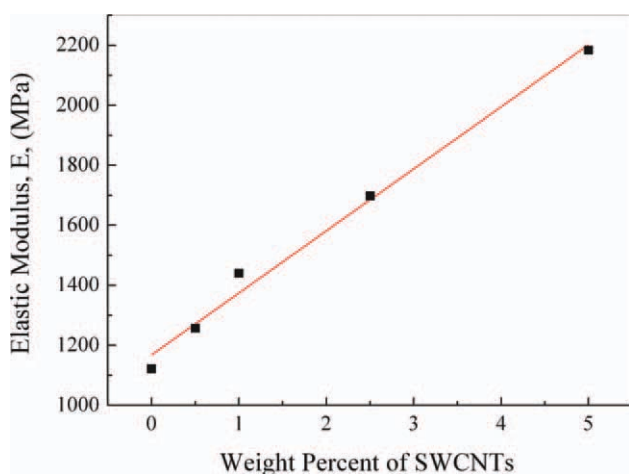


**Figure 15** The dependence of the elastic modulus on SWCNTs content at temperature 22°C. [Color figure can be viewed in the online issue, which is available at [wileyonlinelibrary.com](http://wileyonlinelibrary.com).]

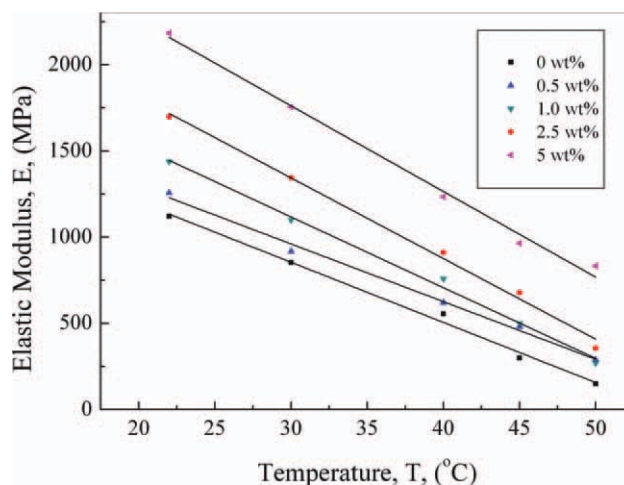


**Figure 16** The dependence of the elastic modulus on temperature for SWCNTs/PVC. [Color figure can be viewed in the online issue, which is available at [wileyonlinelibrary.com](http://wileyonlinelibrary.com).]

value of  $m$  may be considered as an indication of the number of chain's obstacles present.

### CONCLUSIONS

The SWCNTs reinforced PVC samples with different concentrations were prepared by casting technique. The extent of increase in the complex viscosity with increasing SWCNTs content was more pronounced at low frequency when compared with that at higher frequency. It has a percolation concentration threshold of 0.45 wt % of SWCNTs. The storage modulus increases with increasing SWCNTs content and frequency. A gradual decrease in the terminal zone slope of  $G'$  for the nanocomposites with increasing SWCNTs content may be explained by the fact that the nanotube–nanotube interactions will be dominant at higher CNTs content and lead to the formation of the interconnected or network-like structures of SWCNTs in the polymer nanocomposites. The rheological loss factor indicates two relaxation peaks at frequencies of 0.11 and 12.8 Hz. Dynamic mechanical analysis reveals that the height of the  $\tan\delta$  peak declines with the increase of CNTs content, which means an enhancement of the stiffness of the composites. Tensile tests indicate a linear increase in the elastic modulus with increasing CNTs content, while it decreases linearly, too, as the testing temperature increased.

### References

1. Ali Dadfar, S. M.; Alemzadeh, I.; Reza Dadfar, S. M.; Vosoughi, M. *Mater Des* 2011, 32, 1806.
2. Chen, G.; Tian, M.; Guo, S. *J Macromol Sci Phys* 2006, 45, 709.
3. Albayrak, G.; Aydin, I.; *J Macromol Sci Phys* 2008, 47, 260.
4. Gong, F.; Feng, M.; Zhao, C.; Zhang, S.; Yong, M. *Polym Degrad Stabil* 2004, 84, 289.
5. Wan, C.; Qiao, X.; Zhang, Y.; Zhang, Yi. *Polym Test* 2003, 22, 453.
6. Asif, K. M.; Sarwar, M. I.; Rafiq, S.; Ahmad, Z. *Polym Bull* 1998, 40, 583.
7. Xiea, X. L.; Liua, Q. X.; Lic, R. K. Y.; Zhoua, X. P.; Zhang, Q. X.; Yub, Z. Z.; Mai, Y. W. *Polymer* 2004, 45, 6665.
8. Shimpi, N. G.; Verma, J.; Mishra, S. *J Compos Mater* 2010, 44, 211.
9. Zhoul, Y. X.; Wu, P. X.; Cheng, Y. Z.; Ingram, J.; Jeelani, S. *Polym Lett* 2008, 2, 40.
10. Yu, S.; Wong, W. M.; Juay, Y. K.; Yong, M. S. *SIMTech Tech Rep* 2007, 8, 71.
11. Mamunya, Y.; Boudenne, A.; Lebovka, N.; Ibois, L.; Candau, Y.; Lisunova, M. *Compos Sci Tech* 2008, 68, 1981.
12. Gao, L. L.; Chen, X.; Zhang, S. B.; Gao, H. *Mater Sci Eng A* 2009, 513–514, 216.
13. Rocha, N.; Kazlaucinas, A.; Gil, M. H.; Gonçalves, P. M.; Guthrie, T. J. *Compos Appl Sci Manuf* 2009, 40, 653.
14. Zhao, C.; Hu, G.; Justice, R.; Schaefer, D. W.; Zhang, S.; Yang, M.; Han, C. C. *Polymer* 2005, 46, 5125.
15. Kim, S.; Pechar, T. W.; Marand, E. *Desalination* 2006, 192, 330.
16. Cai, H.; Yan, F.; Xue, Q. *Mater Sci Eng A* 2004, 364, 94.
17. Ogasawara, T.; Ishida, Y.; Ishikawa, T.; Yokota, R. *Compos Appl Sci Manuf* 2004, 35, 67.
18. Gojny, F. H.; Wichmann, M. H. G.; Fiedler, B.; Schulte, K. *Compos Sci Tech* 2005, 65, 2300.
19. Koerner, H.; Liu, W.; Alexander, M.; Mirau, P.; Dowty, H.; Vaia, R. A. *Polymer* 2005, 46, 4405.
20. Kuan, H. C.; Ma, C. C. M.; Chang, W. P.; Yuen, S. M.; Wu, H. H.; Lee, T. M. *Compos Sci Tech* 2005, 65, 1703.
21. Seo, M. K.; Park, S. J. *Chem Phys Lett* 2004, 395, 44.
22. Li, C.; Liang, T.; Lu, W.; Tang, C.; Hu, X.; Cao, M.; Liang, J. *Compos Sci Tech* 2004, 64, 2089.
23. Seo, M. K.; Lee, J. R.; Park, S. J. *Mater Sci Eng A* 2005, 404, 79.
24. Kim, J. Y.; Kim, S. H. *J Polym Sci Part B Polym Phys* 2006, 44, 1062.
25. Broza, G.; Piszczek, K.; Schulte, K.; Sterzynski, T. *Compos Sci Tech* 2007, 67, 890.
26. Brostow, W.; *Performance of Plastics*; Hanser Verlag, 2000, 147–178.
27. Lucas, E. F.; Soares, B. G.; Monteiro, E. *Caracterização de Polímeros: Determinação de Peso Molecular e Análise Térmica*; E-Papers Servicos Editoriais, Brasil 2001.
28. Gedde, U. W. *Polymer Physics*; Kluwer Academic Publisher: Dordrecht, 1999.
29. Xu, W. B.; Zhou, Z. F.; Ge, M. L.; Pan, W. P. *J Therm Anal Calorim* 2004, 78, 91.
30. Polaskova, M.; Sedlacek, T.; Kharlamov, A.; Pivokonsky, R.; Saha, P. In *Polymer Processing Society Europe/Africa Regional Meeting*; Cyprus: Larnaca; 2009. p 97.
31. Du, F.; Scogna, R.; Zhou, W.; Brand, S.; Fischer, J.; Winey, K. *Macromolecules* 2004, 37, 9048.
32. Krishnamoorti, R.; Vaia, R.; Giannelis, E. *Chem Mater* 1996, 8, 1728.
33. Fernandez, I.; Santamaria, A.; Munoz, M E.; Castell, P. *Eur Polym J* 2007, 43, 3171.